Radiocarbon dating of seized ivory confirms rapid decline in African elephant populations and provides insight into illegal trade

Thure E. Cerling[a,b,c,1], Janet E. Barnette[a], Lesley A. Chesson[a], Iain Douglas-Hamilton[d,e], Kathleen S. Gobush[f], Kevin T. Uno[g], Samuel K. Wasser[h], and Xiaomei Xu[i]

[a]IsoForensics, Inc., Salt Lake City, UT 84108; [b]Department of Geology and Geophysics, University of Utah, Salt Lake City, UT 84112; [c]Department of Biology, University of Utah, Salt Lake City, UT 84112; [d]Save the Elephants, Nairobi 00200, Kenya; [e]Department of Zoology, University of Oxford, Oxford OX1 3PS, United Kingdom; [f]Wildlife Program, Vulcan, Inc., Seattle, WA 98104; [g]Lamont-Doherty Earth Observatory, Division of Biology and Paleo Environment, Columbia University, Palisades, NY 10964; [h]Center for Conservation Biology, Department of Biology, University of Washington, Seattle, WA 98195; and [i]Department of Earth System Science, University of California, Irvine, CA 92697

Contributed by Thure E. Cerling, September 12, 2016 (sent for review August 4, 2016; reviewed by Edouard Bard and Daryl Codron)

Carbon-14 measurements on 231 elephant ivory specimens from 14 large ivory seizures (≥0.5 ton) made between 2002 and 2014 show that most ivory (*ca*. 90%) was derived from animals that had died less than 3 y before ivory was confiscated. This indicates that the assumption of recent elephant death for mortality estimates of African elephants is correct: Very little "old" ivory is included in large ivory shipments from Africa. We found only one specimen of the 231 analyzed to have a lag time longer than 6 y. Patterns of trade differ by regions: East African ivory, based on genetic assignments of geographic origin, has a much higher fraction of "rapid" transit than ivory originating in the Tridom region of Cameroon–Gabon–Congo. Carbon-14 is an important tool in understanding patterns of movement of illegal wildlife products.

wildlife | forensics | isotopes | Africa | genetics

The illegal trade in elephant ivory has increased significantly in the past decade (1, 2), with studies estimating the current rate of decline of regional African elephant populations to be as high as 8%, primarily due to poaching (3, 4). Central African forest elephant populations decreased by *ca.* 62% from 2002 to 2011 (5). Forest elephants are particularly vulnerable to poaching because of their slow population growth rates compared with their savanna counterparts (6). Savanna elephants have also experienced massive population declines, particularly in Tanzania and northern Mozambique. The savanna elephant population in the Selous Wildlife Reserve in Tanzania saw a 66% decline from 2009 to 2013 (7). The rapid decline in elephants across Africa has been attributed to the high poaching rates and increased amount of ivory seized over the last decade or so (3). Total global seizures in excess of 40 tons of ivory have occurred in several years since 2010 (8), with over 70% of all ivory seizures exceeding 0.5 ton (hereafter termed "large seizures" or "large ivory seizures").

We use "bomb ^{14}C" to determine ages of ivory from 14 different large seizures intercepted by law enforcement officials between 2002 and 2014. These ages represent the date of death of those elephants whose tusks were sampled. This study answers several questions including whether "old" ivory—such as tusks from government stockpiles—is being incorporated into the illegal ivory stream, what the lag time is between animal death and seizure of ivory by law enforcement officials, and whether there are significant differences between the age of ivory originating in different parts of Africa.

We first establish a ^{14}C-calibration relationship for animal tissues from Africa by using elephant hair of known age. We then report 231 ^{14}C-calibrated ages of seized ivory and discuss how these ages influence our understanding of the illegal ivory trade in Africa. We use specimens previously studied by Wasser et al. (2), who assigned ivory to its general location of origin using DNA assignment methods.

Results

Calibration Curve. Carbon-14 is a naturally occurring isotope produced by cosmic radiation in the upper atmosphere. Aboveground nuclear weapons testing, primarily in the early 1960s, nearly doubled the concentration of ^{14}C from the natural abundance level (Fig. 1*B*). Since the atmospheric concentration "spike" of ^{14}C reached at that time, the $^{14}C/^{12}C$ ratio has been steadily declining from peak values of *ca*. 1.95 and *ca*. 1.8 $F^{14}C$ [fraction modern carbon (9)] in the Northern and Southern Hemispheres (NH and SH), respectively, to the current value of < 1.03; this "bomb-curve" record is well-documented (10–16). The overall higher concentration and peak value of atmospheric ^{14}C in the NH was due to higher amounts of testing in the NH compared with the SH. Zonal heterogeneity in concentrations was observed in each hemisphere in the 1960s and early 1970s and, as a result, multiple calibration curves (e.g., NH1, NH2, and NH3 and SH1–2 and SH3) were established for each hemisphere (10–12). Atmospheric ^{14}C is present primarily as $^{14}CO_2$ and the mixing time of CO_2 in the atmosphere is ∼10 y. Thus, by about 1973, the bomb pulse of $^{14}CO_2$ was essentially mixed and zonal differences were insignificant; the NH and SH have been each treated as a single zone since 1973 (12).

Significance

C-14 dating methods can be used to determine the time of death of wildlife products. We evaluate poaching patterns of elephants in Africa by using ^{14}C to determine lag time between elephant death and recovery of ivory by law enforcement officials. Most ivory in recent seizures has lag times of less than 3 y. Lag times for ivory originating in East Africa are shorter, on average, than the lag times for ivory originating in the Tridom region (Cameroon–Gabon–Congo). The ^{14}C data show little or no evidence that large-scale ivory shipments contained ivory stockpiled over long time periods. Little, if any, "old" ivory (i.e., >10 y) seems to contribute to large ivory shipments.

Author contributions: T.E.C., L.A.C., I.D.-H., K.S.G., K.T.U., S.K.W., and X.X. designed research; T.E.C., J.E.B., L.A.C., K.T.U., S.K.W., and X.X. performed research; T.E.C., L.A.C., K.T.U., S.K.W., and X.X. analyzed data; and T.E.C., L.A.C., K.T.U., and S.K.W. wrote the paper.

Reviewers: E.B., Centre de Recherche et d'Enseignement de Géosciences de l'Environnement; and D.C., National Museum, Bloemfontein.

Conflict of interest statement: I.D.-H. is chief executive officer of Save the Elephants, which provided partial funding for this research, and K.S.B. is employed by Vulcan, Inc., which provided partial funding for this research through the Paul G. Allen Family Foundation.

Freely available online through the PNAS open access option.

[1]To whom correspondence should be addressed. Email: thure.cerling@utah.edu.

This article contains supporting information online at www.pnas.org/lookup/suppl/doi:10.1073/pnas.1614938113/-/DCSupplemental.

Table 1. Lag time in months for ivory samples from 14 different seizures, grouped by region of origin, as determined by ^{14}C dating

Name	Abbreviation	Date of seizure	Region of origin	*N*	Mean	±1 σ	Mimimum	Maximum	Median
Avocado	AVO	August 22, 2010	East Africa	14	6	9	−10	15	10
HKTA	HKTA	October 17, 2012	East Africa	11	19	7	11	37	18
HKTB	HKTB	October 17, 2012	East Africa	14	14	6	6	21	12
Hong Kong-Kenya	HKK	January 26, 2013	East Africa	10	14	9	1	27	13
Hong Kong-Nigeria	HKN	August 7, 2013	Tridom	11	21	7	8	30	23
Hong Kong-Togo	HKI	July 18, 2013	Tridom	10	39	11	25	62	38
Malawi	M	May 23, 2013	East Africa	11	20	9	5	35	21
Malaysia*	MYS	December 11, 2012	East Africa	39	23	7	4	39	24
Malaysia*	MYS	December 11, 2012	Tridom	28	35	40	5	231	27
Malaysia*	MYS	December 11, 2012	West Africa	13	19	15	5	67	15
Philippines7	S7	June 9, 2009	East Africa	14	6	6	−4	18	6
Pili	PIL	May 6, 2011	East Africa	10	18	8	3	31	20
Singapore 2002	LAC	June 28, 2002	Zambia	8	15	6	6	25	14
Singapore 2014	SGP	March 27, 2014	East Africa	10	28	7	20	44	27
Taiwan1	53-	July 6, 2006	East Africa	12	15	20	1	69	8
Togo	TOGI	January 29, 2014	Tridom	16	25	11	9	52	22

*The Malaysia 2012 seizure had ivory assigned to three different geographic origins: East Africa, Tridom, and West Africa. Results from these different assignments are listed separately.

However, differences between the NH and SH persist today due in part to the Suess effect, the dilution of ^{14}C in the atmosphere by "dead carbon"—fossil fuels have no radiocarbon and combustion of those fuels dilutes the modern atmosphere with carbon (as CO_2) with an $F^{14}C$ value of 0.0. Most of the dead carbon is produced in the NH and mixes across the equator with the SH in the Inter-Tropical Convergence Zone (ITCZ, shown in Fig. S1*C*); since 1990 this has been the principal driver for differences in $F^{14}C$ between the NH and SH (10–12). The natural exchange of $^{14}CO_2$ between the ocean and atmosphere also contributes to the $F^{14}C$ gradient observed between the NH and SH. Atmospheric samples collected near the equator should have a time–$F^{14}C$ relationship between that of the NH and SH due to mixing across the ITCZ.

Atmospheric ^{14}C (as $^{14}CO_2$) enters the terrestrial biosphere by photosynthesis; ^{14}C is subsequently incorporated into herbivore tissues as the animals ingest plants for food. The bomb-^{14}C signal has been used in human forensic studies (17–21) and has also been used previously to date ivory and other animal tissues including hair, horn, and tooth enamel (22–25). Prior work on ^{14}C dating of ivory has used the atmospheric $^{14}C/^{12}C$ historical record to determine the calibrated age of samples. Both Vogel et al. (23) and Uno et al. (25) note that the $^{14}C/^{12}C$ atmospheric record gives ivory ages that are, in general, 0–2 y earlier than the known age of the sample. This age mismatch likely results from several processes: (*i*) differing $^{14}C/^{12}C$ ratios between the NH and SH compounded by the lack of atmospheric $^{14}CO_2$ measurements in the mixing zone between the hemispheres (i.e., equatorial Africa), (*ii*) the remobilization of nonstructural carbon during plant growth, (*iii*) the time lag between C fixation by plants and ingestion of plants by an elephant, and (*iv*) recycling of proteins in mammals. Each of these is discussed below.

(*i*) Differing $^{14}C/^{12}C$ ratios between hemispheres: Fig. 1*A* shows that the "clean-air" sites of the NH and SH have different values for $F^{14}C$ at any given time. Fig. S1*C* shows that the clean-air sites used to determine $F^{14}C$ of NH and SH are far from the African continent. (*ii*) Remobilization of nonstructural carbon during plant growth: Muhr et al. (26) have shown that nonstructural carbon in perennial tissues (e.g., branches, stems, and roots) can be mobilized and used for growth several years after fixation and thus $F^{14}C$ of dietary foodstuff may lag the $F^{14}C$ of the atmosphere; because elephants have a high component of perennial plants in their diets, this effect could be important in understanding any offset between atmospheric $F^{14}C$ and newly formed tissue $F^{14}C$ in herbivores. Ehleringer et al. (27) showed a significant range in $F^{14}C$ for plants collected at a single time from a single region. (*iii*) Time lag between C fixation by plants and ingestion of plants by an elephant: If carbon in the food that animals eat has been fixed previously, there is likely to be an offset of months or years between the date of ingestion and the date of carbon fixation. This is particularly significant in elephants, because they ingest large quantities of bark and wood, which—if even a small fraction of this carbon is digested and fixed in animal tissues—would skew the ^{14}C-calibrated age to an earlier date. (*iv*) Recycling of proteins in mammals: Ayliffe et al. (28) showed that newly formed proteinaceous animal tissues (e.g., collagen and keratin) are composed of about 45% carbon with a turnover time (half-life) of ∼140 d; thus, proteins should have an "average age" skewed several months before tissue formation.

The combination of these processes may affect the accuracy of age-dating ivory when using the standard NH or SH zonal calibration curves over the past *ca.* 15 y where the slope of the bomb curve is relatively shallow. Therefore, we analyzed 14 elephant hairs with known collection dates between 2001 and 2013 (*Methods*, Table S1, and Fig. S1*B*) to develop a calibration curve specific to elephant tissues. Fig. 1 shows the elephant hair relationship for $F^{14}C$ versus date and also the data for the same time interval used to calculate the NH and SH regions NH3 and SH3, respectively, as reported in ref. 16. Dates were assigned to hairs using the segment length collected for measurement and assuming a growth rate of 0.8 mm/d. We use a linear regression for the period 2001–2013 to derive the relationship $F^{14}C = [-0.0049928 \times \text{year} + 11.09197]$ ($r^2 = 0.988$); we note that this linear relationship should not be used for dates before 1995 (Fig. 1*B*). We assume that the incorporation of ^{14}C from diet into proteinaceous tissue is the same for elephant hair keratin as it is for elephant ivory collagen and thus use the calibration curve to determine the date of death of the elephant from which each seized tusk originated. If a calibration curve can be generated from ivory of known age—and differs significantly from the calibration curve generated from elephant hair—dates can be recalculated using such new data. All of the calibration samples, and the assigned locations of ivory, fall in (or very near to) the mixing zone across the ITCZ, which separate the NH and SH zones where the "clean-air" sites are located. Future calibrations for ivory, or for other wildlife products, to obtain "age" determinations using $F^{14}C$ measurements should focus on obtaining samples near regions of interest; such calibrations will further improve the age estimates of this and other studies.

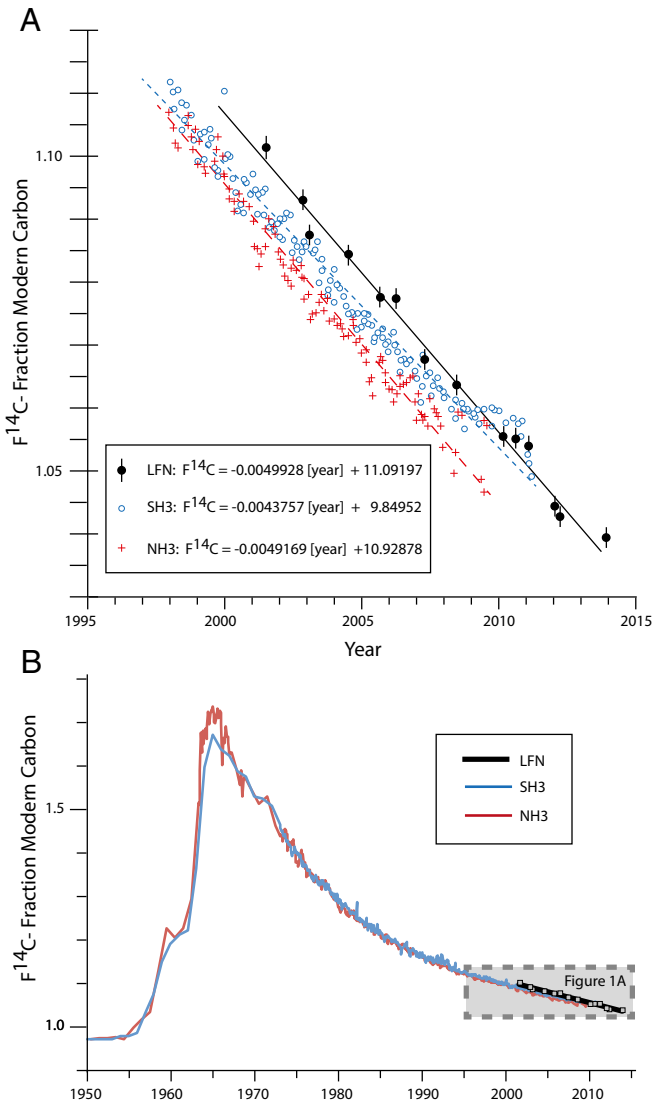

Fig. 1. (*A*) Relationship between $F^{14}C$ and date of collection for elephant hair and for the data used in NH3 and SH3 calibration curves (6). The elephant hair calibration curve is used to calculate date of death from 2001 to 2014. (*B*) The complete "bomb curve" from 1950 to the present for NH3 and SH3. We note that after 1973 all NH zones are treated as a single zone, and all SH zones are treated as a single zone.

Ivory for date-of-death determination was sampled from the pulp cavity of tusks (the proximal end of the tusk; Fig. 2 and Fig. S2), which is where new ivory (dentine) was forming when the elephant died and thus most accurately records the date of death.

Radial Growth Rates of Tusks. For a limited set of tusks we sampled the innermost dentine and also the outermost dentine (Fig. 2 and Fig. S2); in a few cases we also sampled the cementum, which forms outside the outermost dentine. The bomb curve has a "rising" and a "falling" limb: rapidly increasing in the late 1950s, peaking in the early 1960s with the crest in the SH occurring after that in the NH, then gradually diminishing to the current $F^{14}C$ value of *ca.* 1.02 (Fig. 1*B*). Thus, an age assignment using $F^{14}C$ of any postbomb ivory has three solutions, one entirely on the rising limb of the bomb curve (i.e., between *ca.* 1955 and 1965), one with the outer dentine on the rising limb (between 1955 and 1965) and the inner dentine on the falling limb (between 1965 and the present), and one entirely on the falling limb (both after 1965). For ivory entirely on the rising limb, the innermost dentine should have a higher $F^{14}C$ value than the outermost dentine; data from Table S2 show that this is not the case. For the second case, the outermost dentine would have formed between 1955 and 1965 and the innermost dentine would have formed in the last decade, giving unreasonably slow growth rates for ivory (*ca.* 1 cm thickening per 50 y). Our samples fall in the third case, where both the innermost and outermost dentine $F^{14}C$ values are on the falling limb, with the innermost dentine having lower $F^{14}C$ values than the outermost dentine.

All tusks with multiple samples are on the falling limb of the bomb curve, and we thus assume that all other specimens analyzed in this study are on the falling limb. We use the tusks with multiple samples to determine the rate of radial growth of tusks. Radial growth rates were about 7 mm/y for both savanna and forest elephants, ranging from *ca.* 6–14 mm/y (complete results are presented in Table S2 and Fig. S3). Uno et al. (25) measured longitudinal growth rates of *ca.* 5 cm/y for two female African elephants, which correspond to radial growth rates of about 5 mm/y based on a longitudinal/radial growth rate ratio of about 10:1.

Date-of-Death Determinations of Seized Ivory. The $F^{14}C$ values and calculated date of death of 231 ivory specimens (tusks) from 14 large seizures from 2002 to 2014 are summarized in Table 1; complete data are presented in Dataset S1. Details for 12 of the seizures are given in Wasser et al. (2). Two additional seizures were included in our study and were not available at the time of the Wasser et al. (2) study.

Ivory specimens are discussed in the context of lag time, which is the time between when the animals died as determined by $F^{14}C$ using the calibration discussed above and the time of seizure by law enforcement officials. The lag times for each seizure are shown in Fig. 3, where they are grouped by geographic origin based on DNA analysis (2). Uncertainty for the calculated lag time, defined here as the expanded uncertainty (*U*), incorporates uncertainty in the calibration curve (Fig. 1*B*) and measurement reproducibility (Dataset S1 and *Methods*).

Wasser et al. (2) assigned individual ivory specimens to different geographic regions based on genetic data (Fig. S1*A*). Those assignments have an estimated accuracy of approximately ±300 km for both latitude and longitude. Based on those assignments, we group specimens into four distinct regions of origin: East Africa (southern Kenya to northern Mozambique), the Tridom (Cameroon, Republic of Congo, and Gabon, but also including Southwest Central African Republic), West Africa, and

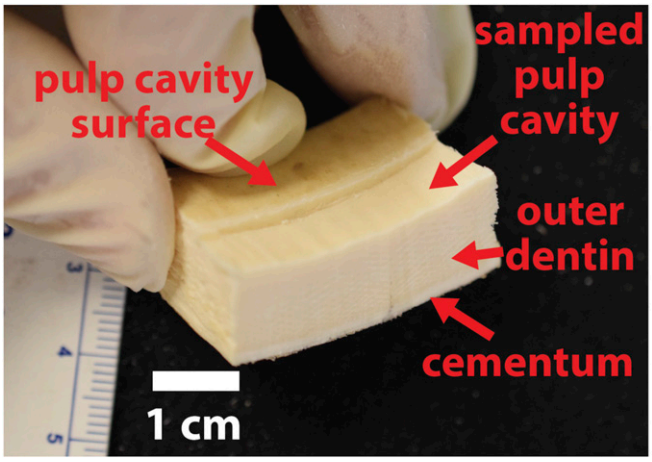

Fig. 2. Example of sample from pulp cavity section of specimen SGP-1-2. Arrows indicate the locations of the pulp cavity surface, a sampled area (~2 mm total depth from the pulp cavity surface), outer dentine, and the cementum layer deposited on the outside of the tusk.

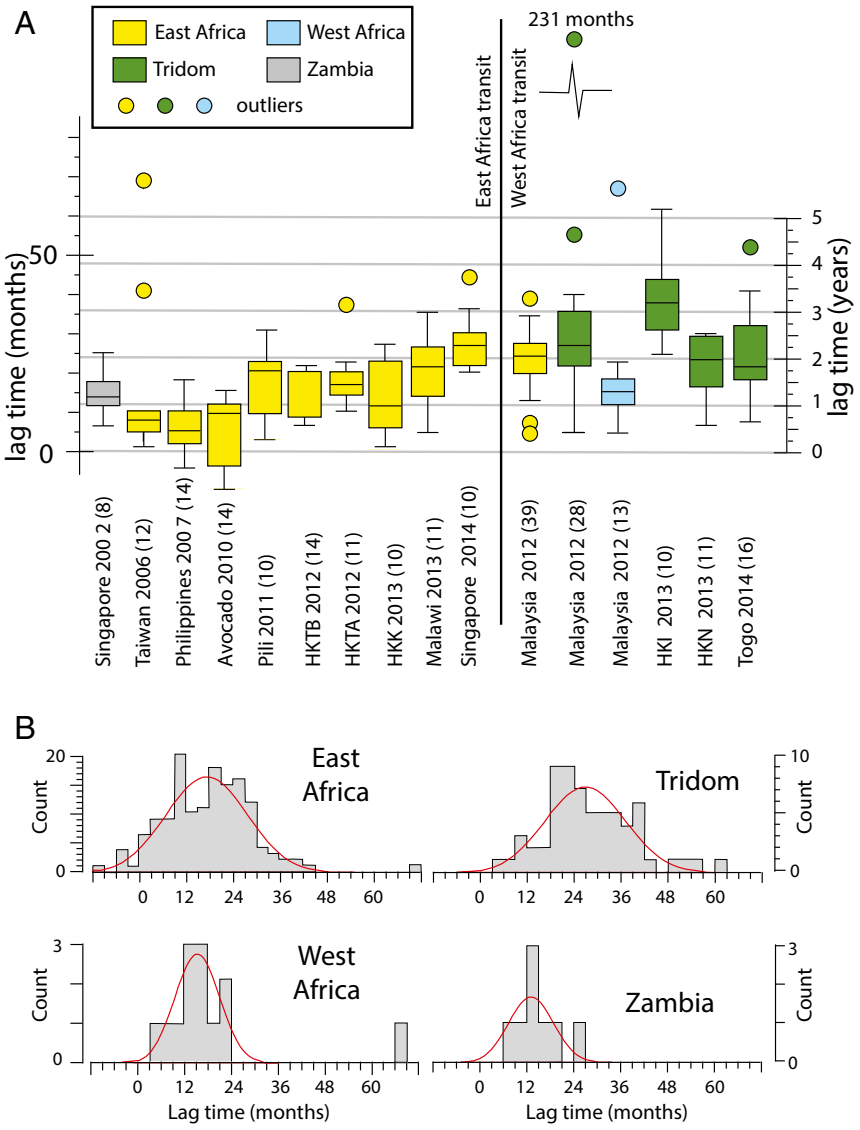

Fig. 3. (*A*) Box and whisker diagram for median lag times (difference between date of death and seizure date) of ivory specimens analyzed in this study; the number of specimens with $F^{14}C$ measurements for each grouping is given in parentheses. (*B*) Histograms showing lag times for specimens from East Africa, Tridom, West Africa, and Zambia. Red lines are the normal distributions for each regions fit to the data (*Methods*).

Zambia. The earliest and largest seizure analyzed (6.5 tons seized in Singapore in 2002) seemed to have primarily a Zambian origin. A seizure from Malaysia (December 2012), the second-largest seizure on record (6 tons), had specimens with assigned origins in West Africa, East Africa, and the Tridom; tusks from different regions within that Malaysian seizure will be discussed in a regional context along with other specimens from those respective regions.

Very Old Ivory in Seizures. Of the 231 individual ivory specimens studied, only one specimen had a lag time greater than 6 y (72 mo) (Fig. 3); this specimen was from the Tridom region and had an estimated lag time of 231 mo (>19 y; uncertainty range is 211–252 mo). Only three other specimens had lag times greater than 5 y (60 mo). In contrast, we would expect ivory originating from long-term stockpiles to date from the present to 1989 or earlier (i.e., with possible lag times of 27 y or greater), coinciding with the international trade ban; such ivory would have a broad distribution of lag times that should range from near zero to tens of years. Thus, it is unlikely that "old" ivory from government or other stockpiles was present in the large ivory seizures we analyzed.

Average Lag Times and Distributions of Ivory Age in Seizures. We consider the lag time for three transit periods: rapid (<12 mo), intermediate (12–24 mo), and slow (>24 mo). Only seizures of ivory originating in East Africa have rapid transit times; 5 of the 10 East African groups had 50% or more of specimens with lag times in the "rapid" category. No seizures from other regions had more than 25% of tested specimens in the rapid transit category (Fig. 4). In contrast, seizures originating in the Tridom were dominated by specimens with intermediate to slow transit times (Fig. 4). Overall, the rapid:intermediate:slow (R:I:S) pattern for lag times in East Africa is 35:41:24 (n = 145), whereas R:I:S is 8:35:57 (n = 65) for the Tridom region. With only a single subgroup from the Malaysian seizure originating in West Africa, and only a single (early) seizure originating in Zambia, it is difficult to make generalizations about the relative proportions of transit times based on the lag time determinations for those regions. Nevertheless, the short lag time of the West Africa ivory is noteworthy given the few remaining elephants there.

Our results suggest that there may be regional differences in lag times at the shipping container level of distinction. However,

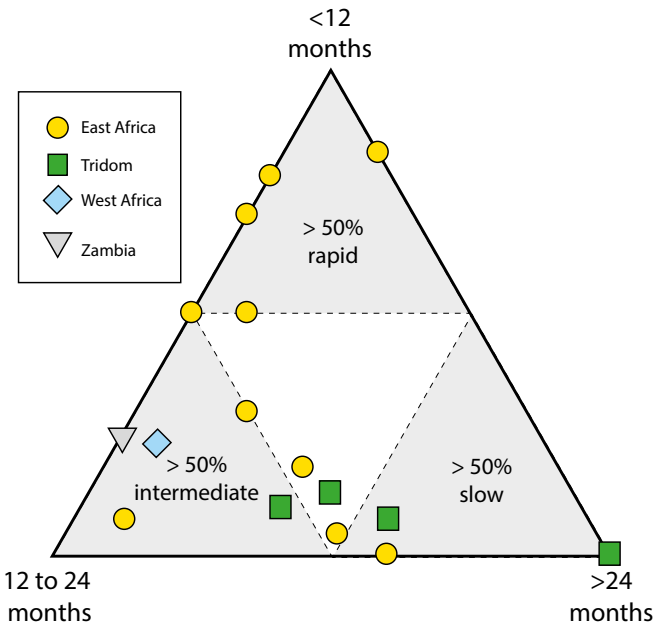

Fig. 4. Lag time distribution shown as a ternary plot for rapid transit (<12 mo lag time), intermediate transit (12–24 mo), and long transit (>24 mo).

we note that the radiocarbon calibration and related uncertainties have large associated errors and that refined regional radiocarbon calibrations may provide better constraints on regional differences in lag times.

Changes in Lag Times from 2002 to 2014. The median lag time for seizures between 2002 and August 2010 ranges from 7 to 13 mo. Lag time increases from 2011 onward, ranging from 13 to 32 mo (Fig. 5). This trend of increasing lag time is most evident in East African seizures where there are a total of nine seizures made over 9 y. The combined dataset from the regions of West Africa ($n = 1$), Southern Africa (Zambia, $n = 1$), and the Tridom ($n = 4$) is smaller than the East Africa dataset but supports the trend of increasing lag time since 2011. The reason for the general increase in lag time since 2011 is unclear. It is likely related to the overall decline in African elephant populations, particularly from 2010 to 2012, where data show population decline due to unsustainable poaching rates, especially in Central and East Africa (3, 4). As a result, it may take longer to accumulate enough large tusks to make a large shipment more profitable. Considering the markedly slower growth rate of tusks of forest elephants, this may also explain the longer lag times we observed for Central African ivory compared with East African ivory. West African forest ivory generally made up a small portion of the tusks in all seizures analyzed and, based on its short lag time, seemed to be added opportunistically at the time of shipment. Factors related to the dynamics of the illegal network of trade or perhaps to changes in the demand for ivory (29, 30) may have also contributed to these trends.

Conclusions

A calibration curve for $F^{14}C$ of modern wildlife tissues in Africa shows that modern elephant hair samples (keratin) have an offset with respect to the bomb curve between about 1 and 2 y from both the NH zone 3 (NH3) and SH zone 3 (SH3) relationships, with the tissue samples having higher $F^{14}C$ values than either the NH3 or SH3 curves. This is likely due to elephant diets that include carbon that was fixed some months to years before ingestion, and also due to recycling of some proteins during keratin or collagen synthesis. The elephant hair calibration curve can be used to determine the date of death of elephants if the $F^{14}C$ of ivory is measured along the pulp cavity of the tusk. It may be necessary to establish taxon-specific calibration curves for date-of-death determinations based on radiocarbon dating of other wildlife products, such as rhinoceros horn, pangolin scales, pelts or furs, or timber. Issues specific to different dietary (i.e., carbon) sources, tissue types, and geographic regions need to be considered for related studies that use $F^{14}C$ measurements to determine the age of wildlife products.

Examination of 231 ivory samples from 14 seizures made between 2002 and 2014 shows that the lag time between elephant death and seizure by law enforcement officials has median values generally ranging between 6 and 35 mo. Specimens originating from East Africa—previously determined via genetic analysis—have the shortest lag times, with *ca*. 35% of specimens having lag times <12 mo; by comparison, only 7% of ivory specimens originating from the Tridom region of Africa have lag times <12 mo. Only a single specimen analyzed in this study has a lag time >10 y: We find no evidence that long-term government or other stockpiles have been contributing significant amounts of ivory to the illegal ivory trade, emphasizing that poached ivory is being rapidly moved into the illegal trade. This study demonstrates the power of bomb-curve radiocarbon dating for revealing lag times between date of death and seizure, a technique that can be applied to seizures of other wildlife parts, providing critical information to law enforcement, conservation, government, and policy organizations and agencies.

Methods

We report elephant hair and ivory ^{14}C measurements in this paper. Ivory specimens were obtained from seizures in Africa and Asia; specimens were ~10-cm^2 blocks obtained from the proximal end of the tusk [see ref. 31 and as illustrated in Fig. S2 (32)]. We sampled the innermost dentine in the pulp cavity for samples used to assign date of death to animals (Fig. 2 and Fig. S2); for selected specimens, we also dated the outermost dentine, which often had an outer sheath of cementum that was sampled. Powder was obtained using a high-speed rotary Dremel tool and double-cut carbide bits from the innermost 1–2 mm of the ivory block. Hair samples were obtained during collaring or translocation operations conducted by Save the Elephants and by the Kenya Wildlife Service. The basal 1 cm of hair was analyzed for DNA markers; the subsequent 2 mm (i.e., from 10 to 12 mm) was used for $F^{14}C$ measurements. Dates were corrected to *ca*. 14 d before the date of collection assuming an average growth rate of 0.8 mm/d (33).

Dentine powder was demineralized with hydrochloric acid to isolate the collagen component; ~1 mg of carbon was used for a single accelerator mass spectrometry (AMS) measurement (*ca*. 10 mg ivory powder). Delipified hair or demineralized collagen was placed into a precombusted quartz tube with precombusted reagents (cupric oxide and silver), sealed under vacuum, and combusted at 850 °C to convert all organic-bound carbon to carbon dioxide gas (CO_2). CO_2 was cryogenically purified and reduced to graphite; graphite from each

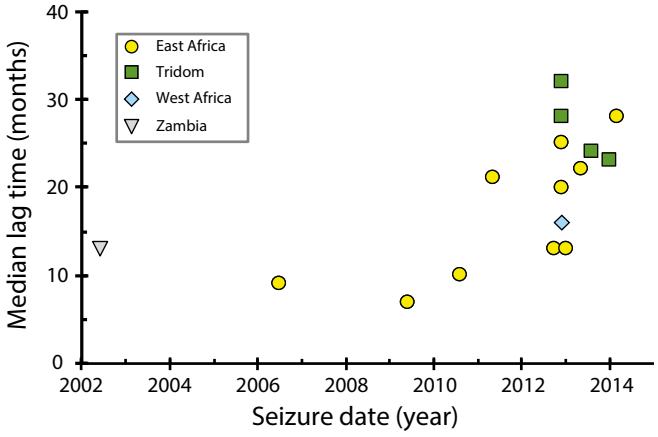

Fig. 5. Median lag time (months) plotted versus seizure date from 2002 to 2014. There seems to be an increase in lag time beginning in 2011.

sample was thereafter pressed into a target for radiocarbon (^{14}C) measurement. The graphite targets were sent to the W. M. Keck Carbon Cycle Accelerator Mass Spectrometry Laboratory at the University of California, Irvine (UCIAMS) for radiocarbon measurement. Radiocarbon results are reported as fraction modern $F^{14}C$ (9), which specifically includes $\delta^{13}C$ normalization to –25% using the AMS measured $\delta^{13}C$ value.

Expanded uncertainty in lag time incorporates uncertainty in the calibration curve (Fig. 1*B*) and in measurement reproducibility. The latter is estimated by specimen "ivory_Modern 207," a homogenized powdered ivory sample prepared multiple times (e.g., separate rounds of collagen extraction, combustion, graphitization, and $F^{14}C$ measurement) and analyzed within each analytical sequence. Ten analyses of ivory_Modern 207 gave an average $F^{14}C$ value of 1.1021 ± 0.0032 (1 σ) (Dataset S1). *U* is calculated from a linear combination of this measurement uncertainty and predicted values from the elephant hair calibration curve, multiplied by a coverage factor (*k*) of 2, which represents *ca*. 95% uncertainty for the range in lag times. For seized specimens with measured $F^{14}C$ values similar to those of the elephant hair used to build the calibration curve (e.g., $F^{14}C \leq 1.1043$), *U* was ± 1.55 y (± 18.5 mo). One seized ivory specimen had an $F^{14}C$ value of 1.1379; *U* for this specimen ("ivory_200;" see Dataset S1) was calculated as ± 1.71 y (± 20.6 mo). Collagen extracted from a fossil bone was used as a blank for AMS measurement (Dataset S1).

Normal distributions to histograms of lag times (Fig. 3) were fit using JMP (SAS Inst., Inc.).

ACKNOWLEDGMENTS. We thank Tara Wilson for help processing the seizures for analysis, Mark Franklin for help with sampling of ivory specimens for radiocarbon dating, and John Howa and Michael Lott for help with expanded uncertainty calculations. We also thank Edouard Bard, Daryl Codron, and Susan Trumbore for helpful comments on the manuscript. This work was funded by Paul G. Allen Family Foundation Grant 11811 and by the Save the Elephants and Wildlife Conservation "Elephant Crisis Fund." Hair calibration samples were imported with CITES permits US831854, US053837/9, US159997/9, US08996A/9; ivory samples were imported under permits 04US082567/9 and US03172A/9. The following governments agreed to provide samples from their ivory seizures: Malaysia, Thailand, the Philippines, Singapore, Cameroon, Taiwan, Hong Kong, Kenya, Uganda, Sri Lanka, Malawi, and Togo.

1. United Nations Office of Drugs and Crime (2014) Guidelines for methods and procedures of ivory sampling and laboratory analysis (United Nations Office of Drugs and Crime, New York).
2. Wasser SK, et al. (2015) Genetic assignment of large seizures of elephant ivory reveals Africa's major poaching hotspots. *Science* 349(6243):84–87.
3. Wittemyer G, et al. (2014) Illegal killing for ivory drives global decline in African elephants. *Proc Natl Acad Sci USA* 111(36):13117–13121.
4. Chase MJ, et al. (2016) Continent-wide survey reveals massive decline in African savannah elephants. *PeerJ* 4:e2354.
5. Maisels F, et al. (2013) Devastating decline of forest elephants in central Africa. *PLoS One* 8(3):e59469.
6. Turkalo AK, Wrege PH, Wittemyer G (2016) Slow intrinsic growth rate in forest elephants indicates recovery from poaching will require decades. *J Appl Ecol*, 10.1111/1365-2664.12764.
7. Bennett EL (2015) Legal ivory trade in a corrupt world and its impact on African elephant populations. *Conserv Biol* 29(1):54–60.
8. CITES (Convention on International Trade in Endangered Species of Wild Fauna and Flora) (2014) Elephant conservation, illegal killing and ivory trade. SC65 Doc. 42.1. Available at cites.org/sites/default/files/eng/com/sc/65/E-SC65-42-01_2.pdf. Accessed July 1, 2016.
9. Reimer PJ, Brown TA, Reimer RW (2004) Discussion: Reporting and calibration of post-bomb ^{14}C data. *Radiocarbon* 46(3):1299–1304.
10. Hua Q, Barbetti M (2004) Review of tropospheric bomb C-14 data for carbon cycle modeling and age calibration purposes. *Radiocarbon* 46(3):1273–1298.
11. Hua Q, Barbetti M (2007) Influence of atmospheric circulation on regional $^{14}CO_2$ differences. *J Geophys Res* 112(D19):D19102.
12. Hua Q, Barbetti M, Rakowski AZ (2013) Atmospheric radiocarbon for the period 1950-2010. *Radiocarbon* 55(4):2059–2072.
13. Levin I, et al. (2010) Observations and modelling of the global distribution and long – term trend of atmospheric $^{14}CO_2$. *Tellus B Chem Phys Meterol* 62(1):26–46.
14. Levin I, Kromer B, Hammer S (2013) Atmospheric $\Delta^{14}CO_2$ trend in Western European background air from 2000 to 2012. *Tellus B Chem Phys Meterol* 65:1–7.
15. Reimer PJ, et al. (2013) IntCal13 and Marine13 radiocarbon age calibration curves 0-50,000 years cal BP. *Radiocarbon* 55(4):1869–1887.
16. Reimer PJ, Reimer R (2016) CALIBomb. Available at calib.qub.ac.uk/CALIBomb/. Accessed June 25, 2016.
17. Spalding KL, Buchholz BA, Bergman LE, Druid H, Frisén J (2005) Forensics: Age written in teeth by nuclear tests. *Nature* 437(7057):333–334.
18. Cook GT, Dunbar E, Black SM, Sheng X (2006) A preliminary assessment of age at death determination using the nuclear weapons testing ^{14}C activity of dentine and enamel. *Radiocarbon* 48(3):305–313.
19. Ubelaker DH, Buchholz BA, Stewart JEB (2006) Analysis of artificial radiocarbon in different skeletal and dental tissue types to evaluate date of death. *J Forensic Sci* 51(3):484–488.
20. Wang N, et al. (2010) Improved application of bomb carbon in teeth for forensic investigation. *Radiocarbon* 52(2):706–716.
21. Alkass K, et al. (2013) Analysis of radiocarbon, stable isotopes and DNA in teeth to facilitate identification of unknown decedents. *PLoS One* 8(7):e69597.
22. Geyh MA (2001) Bomb radiocarbon dating of animal tissues and hair. *Radiocarbon* 43(2B):723–730.
23. Vogel JC, Fuls A, Visser W (2002) Accurate dating with radiocarbon from the atom bomb tests. *S Afr J Sci* 98:437–438.
24. Sideras-Haddad E, Brown T (2002) Dating studies of elephant tusks using accelerator mass spectrometry. *Proceedings of the Ninth International Conference on Accelerator Mass Spectrometry* (Elsevier, New York).
25. Uno KT, et al. (2013) Bomb-curve radiocarbon measurement of recent biologic tissues and applications to wildlife forensics and stable isotope (paleo)ecology. *Proc Natl Acad Sci USA* 110(29):11736–11741.
26. Muhr J, et al. (2016) How fresh is maple syrup? Sugar maple trees mobilize carbon stored several years previously during early springtime sap-ascent. *New Phytol* 209(4):1410–1416.
27. Ehleringer JR, et al. (2011) ^{14}C calibration curves for modern plant material from tropical regions of South America. *Radiocarbon* 53(4):585–594.
28. Ayliffe LK, et al. (2004) Turnover of carbon isotopes in tail hair and breath CO_2 of horses fed an isotopically varied diet. *Oecologia* 139(1):11–22.
29. Gao Y, Clark S (2014) Elephant ivory trade in China: Trends and drivers. *Biol Conserv* 180:23–30.
30. Gao Y, et al. (2016) Rhino horn trade in China: An analysis of the art and antiques market. *Biol Conserv* 201:343–347.
31. Wasser SK, et al. (2007) Using DNA to track the origin of the largest ivory seizure since the 1989 trade ban. *Proc Natl Acad Sci USA* 104(10):4228–4233.
32. Fisher DC, Fox DL (2007) Season of death of the Dent mammoths. *From the Dent Prairie to the Peaks of the Rockies: Recent Paleoindian Research in Colorado*, eds Brunswig RH, Pitblado BL (Univ of Colorado Press, Boulder, CO), pp 123–153.
33. Wittemyer G, Cerling TE, Douglas–Hamilton I (2009) Establishing longitudinal diet chronologies from isotopic profiles in serially collected animal tissues: An example using tail hairs from African elephants. *Chem Geol* 267:3–11.

Supporting Information

Cerling et al. 10.1073/pnas.1614938113

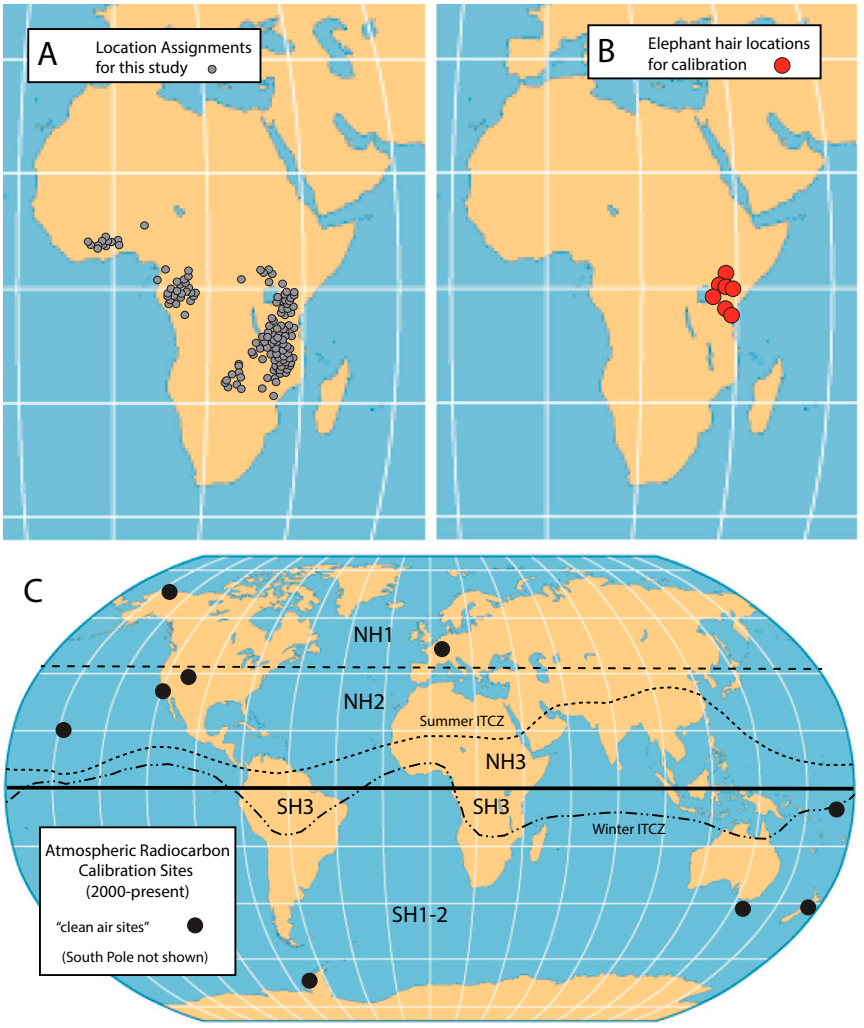

Fig. S1. (*A*) Map of Africa showing location assignments of specimens (from ref. 2) with measured $F^{14}C$ on ivory from the pulp cavity surface. (*B*) Map of Africa showing the locations of samples of elephant hair used for calibration of $F^{14}C$ for elephant tissues. (*C*) Global map showing locations of "clean-air" sites used for calibration of the NH zones (NH1, NH2, and NH3) and SH zones (SH1–2 and SH3) for the period from 2000 to 2013; NH3 and SH3 are bounded by the northern and southern limits of the Inter-Tropical Convergence Zone (following ref. 12 for NH and SH boundaries).

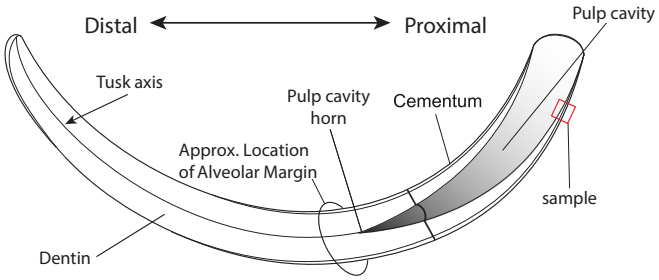

Fig. S2. Schematic of elephant ivory showing longitudinal cross-section of a tusk with pulp cavity, dentine, and cementum. Samples (as shown in Fig. 2) were taken from the proximal end to include the pulp cavity, where the thickness from pulp cavity to the outer cementum sheath was less than 2 cm. Modified from Fisher and Fox (32) with permission from University Press of Colorado.

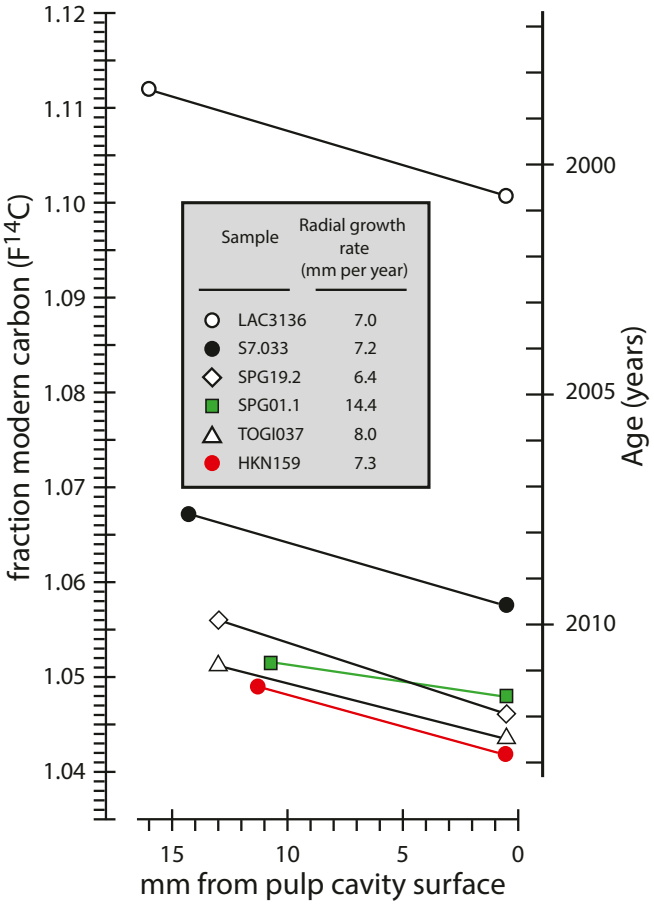

Fig. S3. $F^{14}C$ and thickness relationships for innermost and outmost dentine measured for six elephant tusks in this study. Sample thicknesses were between 1 and 2.5 mm; absolute distances between innermost and outermost samples ranged from 10 to 16 mm.

Table S1. Carbon-14 data for calibration curve from elephant hair collected on known dates

	Sample ID					Date		$F^{14}C$		
Field ID	Latitude	Longitude	IsoForensics ID	UCIAMS no.	Julian	Decimal	Tissue	$F^{14}C$	(1 σ)	Average
STE-010709-Thoreau	0.6	37.5	ivory_214	171243	09.Aug.2001	2001.521	2001.482	1.1012	0.0018	
STE-010709-Thoreau	0.6	37.5	ivory_214	171244	09.Aug.2001	2001.521	2001.482	1.1017	0.0016	1.1014
STE-021030–148:490	0.0	38.3	ivory_216	173827	30.Oct.2002	2002.830	2002.792	1.0930	0.0016	1.0930
STE-030207-Loidaiga	0.2	37.4	ivory_217	173828	07.Feb.2003	2003.104	2003.066	1.0874	0.0016	1.0874
STE-040722-Anastasia	0.6	37.5	ivory_218	173829	22.Jul.2004	2004.557	2004.519	1.0842	0.0017	1.0842
KWS-050828–2 Shimba	−4.3	39.4	ivory_219	171245	26.Aug.2005	2005.652	2005.614	1.0776	0.0016	1.0776
STE-060419-Grace	0.6	37.5	ivory_220	173830	19.Apr.2006	2006.299	2006.260	1.0773	0.0016	1.0773
STE-070425-Sora	2.3	38.0	ivory_221	173831	25.Apr.2007	2007.315	2007.277	1.0678	0.0016	1.0678
STE-080613-Shadrack	2.3	38.0	ivory_224	173833	13.Jun.2008	2008.451	2008.412	1.0637	0.0016	1.0637
STE-100221-Anabelle	0.6	37.5	ivory_226	173834	21.Feb.2010	2010.142	2010.104	1.0556	0.0016	1.0556
STE-100807-Kisima	0.1	37.6	ivory_227	173836	07.Aug.2010	2010.600	2010.562	1.0551	0.0016	1.0551
KWS-LFN-862	−1.6	35.2	ivory_228	173837	04.Feb.2011	2011.096	2011.058	1.0539	0.0018	1.0539
KWS-LFN-853	0.5	36.6	ivory_230	171247	11.Jan.2012	2012.030	2011.992	1.0442	0.0016	
KWS-LFN-853	0.5	36.6	ivory_230	171248	11.Jan.2012	2012.030	2011.992	1.0443	0.0016	1.0443
KWS-LFN-847	−3.4	38.0	ivory_231	173838	25.Mar.2012	2012.232	2012.194	1.0428	0.0015	1.0428
STE-131030-Mtn Bull	0.3	36.8	ivory_232	173839	30.Oct.2013	2013.830	2013.792	1.0395	0.0015	1.0395

Date (tissue) is the estimated age for the integrated sample used for $F^{14}C$ measurement (samples were from 10 to 12 mm from proximal end of hair; assume 0.8 mm/d growth). Data from elephant hair samples used for calibration to establish the relationship between $F^{14}C$ and year of tissue growth for African elephants.

Table S2. Radial tusk growth rates calculated from multiple carbon-14 analyses of ivory

Sample	UCIAMS no.	Distance, mm	$F^{14}C$	1 σ	Year	Rate, mm/y
S7.033_id	167289	0.5	1.0574	0.0016	2009.8	
S7.033_od	167292	14.3	1.0671	0.0016	2007.9	7.2
LAC3136_id	169673	0.5	1.1007	0.0017	2001.2	
LAC3136_od	169675	16.0	1.1118	0.0018	2000.6	7.0
SGP01.1_id	169651	0.5	1.0477	0.0016	2011.7	
SGP01.1_od	169650	10.8	1.0513	0.0016	2011.0	14.4
SGP19.2_id	169664	0.5	1.0461	0.0017	2012.0	
SGP19.2_od	169663	13.0	1.0560	0.0016	2010.1	6.4
TOGI037_id	170313	0.5	1.0435	0.0020	2012.5	
TOGI037_od	170312	13.0	1.0514	0.0016	2011.0	8.0
HKN159_id	170292	0.5	1.0416	0.0019	2012.9	
HKN159_od	170291	11.5	1.0491	0.0016	2011.4	7.3

"id" and "od" represent the innermost and outermost dentine, respectively. $F^{14}C$ data of selected ivory samples with thickness >10 mm for innermost (along pulp cavity) and outermost (inside of cementum) dentine. Age of ivory formation calculated using the elephant hair calibration curve (Fig. 1; Table S1).

Dataset S1. $F^{14}C$ data tables for (1) seized ivory specimens and for (2) replicates and blanks

Dataset S1